

## Original Article

# **In vitro preparation and characterization of dual biomimetic electrospun Wharton's Jelly-derived extra cellular matrix/polycaprolactone sub-micron fibrous band-aid for superior Achilles tendon recovery**

Penghao Li<sup>1,2</sup>, Shuyun Liu<sup>1</sup>, Jingxiang Huang<sup>1</sup>, Jiang Peng<sup>1</sup>, Shibi Lu<sup>1</sup>, Quanyi Guo<sup>1</sup>

<sup>1</sup>Beijing Key Laboratory of Regenerative Medicine in Orthopaedics, Key Laboratory of Musculo-Skeletal Trauma & War Injuries, PLA, Institute of Orthopaedics, Chinese PLA General Hospital, Beijing, China; <sup>2</sup>College of Medicine, Nankai University, Tianjin, China

Received April 21, 2017; Accepted June 23, 2017; Epub August 15, 2017; Published August 30, 2017

**Abstract:** Achilles tendon rupture (ATR) is a common sports injury, and complications usually occur. Promoting self-healing and suppressing the formation of scars and adhesions are priorities when treating ATR. The dual biomimetic electrospun Wharton's Jelly (WJ)-derived extra cellular matrix (ECM)/polycaprolactone (PCL) sub-micron fibrous band-aid was developed for this purpose. Each electrospun band-aid was prepared into two layers: the outer layer was made of ordered PCL fibers and the inner layer was made of ordered PCL and 0%, 25%, 50% or 75% WJ-derived ECM mixed fibers. The ingredients, microstructure, hydrophilicity, and cell adherence and survival were tested. Histological and immunohistochemical staining showed that WJ-derived ECM comprised type I collagen, and the cell nucleus was removed by a special decellularizing process. Fourier transform-infrared spectroscopy (FT-IR) verified the presence of protein in the electrospun band-aids. The electrospun PCL layer had high hydrophobicity and parallel, compact micron-size fibers that decreased viability of L929 cells and inhibited adherence. Electrospun PCL with different ratios of the WJ-derived ECM layer had good hydrophilicity and parallel, loose micron-size fibers. The ability to promote cell adherence and proliferation of the internal surface was 50% ECM > 0% ECM > 25% ECM > 75% ECM. Based on these results, the electrospun band-aid with 50% WJ-derived ECM might eliminate complications and result in superior recovery after ATR.

**Keywords:** Achilles tendon rupture, Wharton's Jelly-derived extra cellular matrix, electrospinning, in vitro, ingredient and microstructure simulation

## Introduction

ATR is one of the most frequent foot and ankle injuries. About 18 people per 100,000 suffer from ATR each year, with middle-aged males (30-50 years) and elderly females (60-80 years) being particularly likely to be affected [1, 2]. Vigorous exercise and progressive degeneration are the foremost causes of ATR [3]. Early effective treatment (< 4 weeks), including conservative treatment, open surgery, or minimally invasive surgery (percutaneous surgery) [3] is indispensable to avoid chronic ATR and restore patients' movement function [4]. However, complications such as re-rupture and adhesions may prevent recovery of the Achilles tendon after treatment [5-8]. Although early post-

operative rehabilitation, advanced surgical techniques, and equipment are available in the clinic [9, 10], repair of Achilles tendons needs to be fundamentally improved.

The self-healing mechanism of ATR is the source of the complications. The self-healing process of the Achilles tendon includes endogenous and exogenous repair activated after ATR (**Figure 1**). The endogenous process involves the recruitment of tenocytes and expression of type I collagen, which produces a tough, naturally composed structure. The exogenous process involves collection of fibroblasts and prevention of fibrosis, which results in scar tissue and peritendinous adhesions [11, 12]. Bio-active substances, such as cytokines and hyal-

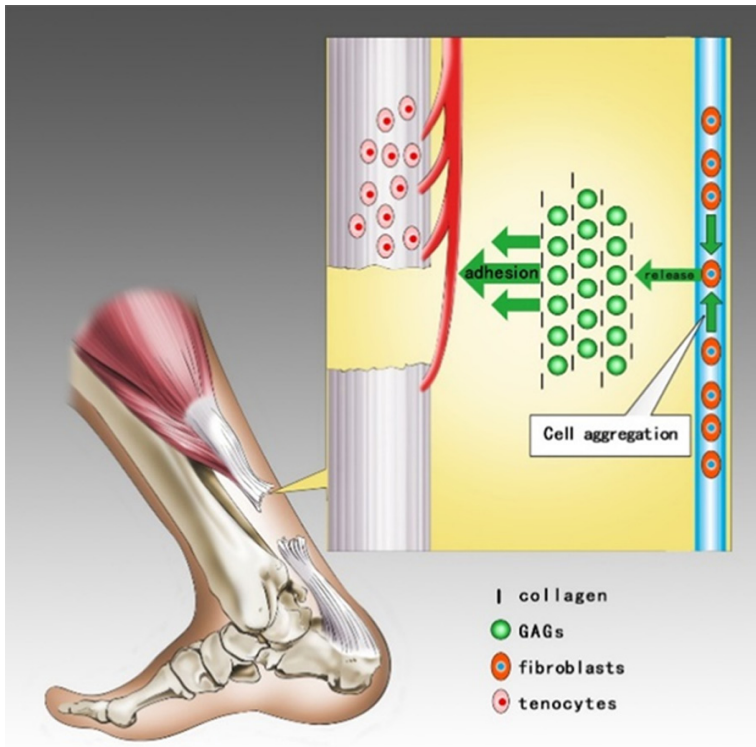


**Figure 1.** Endogenous and exogenous repair mechanisms are activated after an ATR. The endogenous process involves recruitment of tenocytes and expression of collagen I mainly, which relies on blood supply from paratenon and produces a tough structure of natural composition. The exogenous process involves collecting fibroblasts in paratenon, releasing collagens and GAGs and leads to fibrosis between paratenon and Achilles tendon, which results in peritendinous adhesions.

uronic acid (HA), have been used to promote endogenous repair [13-15], whereas drugs and physical barriers, such as celecoxib and polylactic-co-glycolic acid (PLGA), have been utilized to inhibit exogenous repair in the laboratory [16-18]. Our research team has developed the “Achilles tendon band-aid”, a dual biomimetic electrospun WJ-derived ECM/(PCL) sub-micron fibrous membrane, with expected superior effects for Achilles tendon recovery in the clinic.

ECM, which is widely used to repair musculoskeletal defects, has unique ingredients, microstructure, and functions, and it provides a suitable microenvironment for cell metabolism and signal delivery [19-21]. WJ is a firm mucoid connective tissue comprising collagen, hyaluronan, and sulfated glycosaminoglycans (GAGs) that surrounds umbilical cord vessels [22, 23]. The components of WJ are similar to those of the Achilles tendon; however, the proportions of ingredients differ.

After a decellularization process, the WJ-derived ECM has a loose spongy structure with a large number of internal spaces [23]. Electrospinning technology is applied to arrange the ingredients, making it similar to the collagen network in the Achilles tendon. Electrospinning technology is a common method to weave objects with nanofibers, and almost all macromolecular organic matter can be woven using this technology [24], even ECM [25]. The WJ-derived ECM with similar ingredients and microstructure as the Achilles tendon promotes adhesion, proliferation, and differentiation of tenocytes [26]. WJ is a wasted human tissue, and one’s own WJ can be used without any immunological rejection when trauma occurs.

Biocompatibility, biodegradability, stability, and mechanical properties are necessary characteristics of a physical barrier. PCL is a widely used biomedical polymer because

it has all of these properties [27]. Researchers have electrospun a PCL membrane as an outer layer to prevent peritendinous adhesions, and *in vivo* tests have verified the anti-adhesion ability of electrospun PCL membranes [24, 27, 28]. However, the high hydrophobicity and stiffness of PCL may limit its application [29]. The problem can be solved by combining PCL with the ECM, which is hydrophilic and supple.

Complications of ATR treatment, such as re-rupture and peritendinous adhesions, reduce the quality of life and increase the economic burden of patients. Therefore, we prepared and tested the dual biomimetic electrospun WJ-derived ECM/PCL sub-micron fibrous band-aid with 0%, 25%, 50%, and 75% ECM. We compared the WJ ingredients before and after a decellularization process and tested the ingredients, hydrophilicity, and inner surface microstructure of the four kinds of samples. We evaluated adherence and proliferation of fibroblasts

on each sample *in vitro* to realize the band-aids' effects on Achilles tendon recovery.

### Materials and methods

#### *WJ-derived ECM preparation*

Umbilical cords were obtained from 5 women without any systemic diseases who underwent term cesarean deliveries. The informed consents were signed by the maternity patients before the cesarean deliveries. The umbilical cords were handled under aseptic conditions and prepared as follows. This study was approved by Ethics Committee at Chinese PLA General Hospital.

Briefly, the umbilical cords were cut into 15-cm segments and put into vessels, then sent immediately to the laboratory in an ice bath. Distilled water and a small volume of 3% H<sub>2</sub>O<sub>2</sub> were added to rinse, sterilize, and remove floating blood for 30 min. Then the umbilical cords were cut into 3-cm segments, the blood vessels and amniotic membrane were removed, and the WJ was collected. The WJ was minced into a homogenate using a tissue disintegrator. The homogenate was subjected to differential centrifugation from 1,000 rpm to 6,000 rpm at 4°C in a high-speed refrigerated centrifuge (Allegra X-22R refrigerated centrifuge; Beckman, Fullerton, CA, USA), and the WJ-derived ECM was recovered from the supernatant. After that, the supernatant was centrifuged at 10,000 rpm and 4°C. The final sediment was the WJ-derived ECM. The WJ-derived ECM was preserved at -20°C for 30 min, dehydrated completely in a freeze dryer, and lyophilized for 48 h under vacuum. We used only physical methods to remove the cells in the WJ.

#### *Electrospun WJ-derived ECM/PCL band-aid preparation*

To prepare the 2% (w/w) WJ-derived ECM electrospinning solution, 1.3 g ECM was dissolved in 40 ml hexafluoroisopropanol (HFIP) solvent. To prepare 8% (w/w) PCL electrospinning solution, 5.6 g PCL was dissolved in 40 ml HFIP solvent. The 0%, 25%, 50%, and 75% (w/w) WJ-derived ECM/PCL mixture electrospinning solutions were prepared and homogenized by stirring at high speed. The electrospinning solutions were subjected to the same parameters:

voltage, 20 kV; spin length, 10 cm; and flow rate, 0.1 mL/min. The electric force field overcame the surface tension at the needle tip and sprayed into the collector, which was coated with silver paper and rotated at high speed in the form of filaments. The outer layer of the band-aid was fabricated with 5 ml 8% (w/w) PCL electrospinning solution. Then, the inner layer of the band-aid was fabricated with 5 ml 0%, 25%, 50%, or 75% (w/w) WJ-derived ECM/PCL electrospinning solution. After desiccation for 24 h, the dual biomimetic electrospun WJ-derived ECM/PCL sub-micron fibrous band-aids were collected in separate unfiled pouches.

#### *Histological and immunohistochemical staining*

The untreated umbilical cord segments (UUCS) and avascular umbilical cord segments (AUCS) were fixed in 4% formalin solution for 1 week. Then, these segments were dehydrated, embedded in paraffin, sliced to 5- $\mu$ m thickness, and dewaxed at 60°C for 2 h. The WJ-derived ECM was fixed in 4% formalin solution for 30 min and cut into 10- $\mu$ m-thick frozen sections.

Hematoxylin and eosin (H&E) staining was performed to observe the cell morphology and cell distribution of the UUCS, AUCS, and WJ-derived ECM. DAPI stain was used to verify the decellularization effect. Masson's stain and Sirius Red stain were used to observe the arrangement of collagen fibers. Immunohistochemical staining for collagen I, collagen II, and aggrecan was carried out. No antigen retrieval process was used. The sections were stained with primary antibodies to collagen I (1:100; rabbit #ab34710; Abcam, Cambridge, MA, USA), collagen II (1:200; rabbit #ab34712; Abcam), and aggrecan (1:500; mouse #ab3778; Abcam) at 4°C overnight. The sections were incubated in secondary antibodies for 60 min. All images were taken from an inverted fluorescence microscope.

#### *FT-IR analysis*

FT-IR (Tensor 27; Bruker, Ettlingen, Germany) was used to detect the ingredients in the electrospun WJ-derived ECM/PCL sub-micron fibrous band-aids with 0%, 25%, 50%, and 75% ECM, and to detect differences among the four

## Electrospun ECM/PCL band-aid for ATR

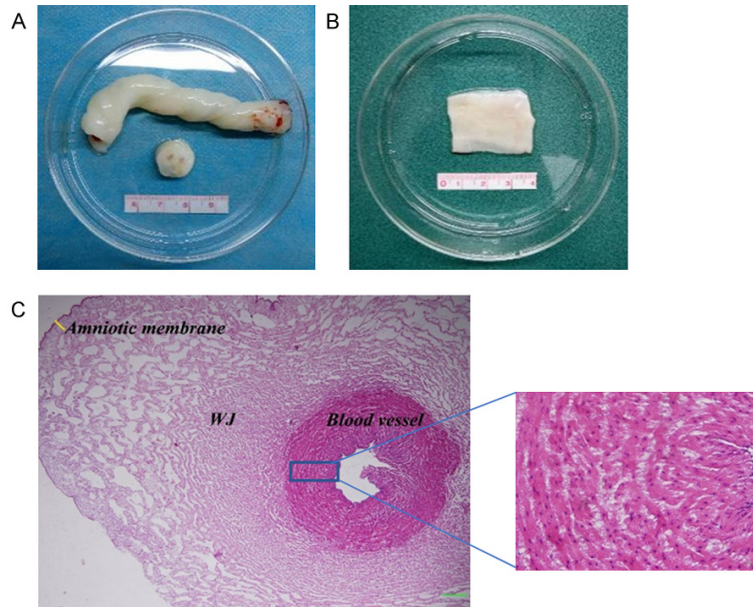


**Figure 2.** The general observation and micro-examination of human umbilical cord. The general observation of human umbilical cord (A). WJ (B). and the micro-examination of human umbilical cord,  $\times 100$  (C).

groups. Flakelets ( $1 \times 1$  cm) with flat surfaces were cut out from each group's electrospun band-aid and were used to conduct the FT-IR analysis. The entire spectra were obtained between  $4000 \text{ cm}^{-1}$  and  $650 \text{ cm}^{-1}$  felicitously.

### Scanning electron microscopic (SEM) analysis

SEM (S-4800; Hitachi, Tokyo, Japan) was used to observe the microstructures of the four electrospun band-aid groups. Flakelets ( $1 \times 1$  cm) with flat surfaces from each group were immobilized on a metal support and sputtered with gold. The scan parameters were 5,000 eV and 0.01 A. The diameters of the electrospun fibers were measured using Image J software (National Institutes of Health, Bethesda, MD, USA).

### Water contact angle (WCA) analysis

The hydrophilic surfaces of each group's electrospun band-aids were assessed by WCA measurements. After a drop of water was added to the surface, the WCA was calculated and plotted automatically with software.

### MTT assay

Approximately  $5 \times 10^4/\text{ml}$  mouse L929 fibroblasts were seeded on a 24-well plate contain-

ing a  $1 \times 1 \text{ cm}^2$  electrospun band-aid and cultured in 1 ml low-glucose Dulbecco's Modified Eagle Medium (DMEM) with 10% fetal bovine serum (FBS) for 24 h. On days 1 and 4, 1 ml MTT was added to all wells of the 24-well plate and incubated for 4 h. Then, the electrospun band-aid was transferred to a new 24-well plate, and 1 ml DMSO was added. After 10 min shock, 0.3 ml of the solution was transferred to a 96 well plate, and the optical density values were measured by a spectrophotometer (Beckman, Fullerton, CA) at 570 nm.

### Statistical analysis

Data are expressed as mean  $\pm$  standard deviation. One-way analysis of variance followed by Bonferroni's multiple-comparison test was used to detect differences between groups, and  $P < 0.05$  was considered significant.

## Results

### General observations and micro-examination of the human umbilical cord

The human umbilical cord was corkscrewed and displayed three main structures: the amniotic membrane, WJ, and umbilical vessels (**Figure 2A**). After the amniotic membrane and umbilical vessels were removed, the WJ was a smooth and viscous slice (**Figure 2B**). The H&E staining results showed that the amniotic membrane was the extremely thin outermost layer; the umbilical vessels were thick and full of cells; and the WJ was observed in the spaces between, surrounded by blood vessels (**Figure 2C**).

### Histological and immunohistochemical staining

Before decellularization, DAPI fluorescent staining revealed that the nuclei (double-stranded DNA) stained blue, and were distributed sporadically in the WJ (**Figure 3A**). The Masson's

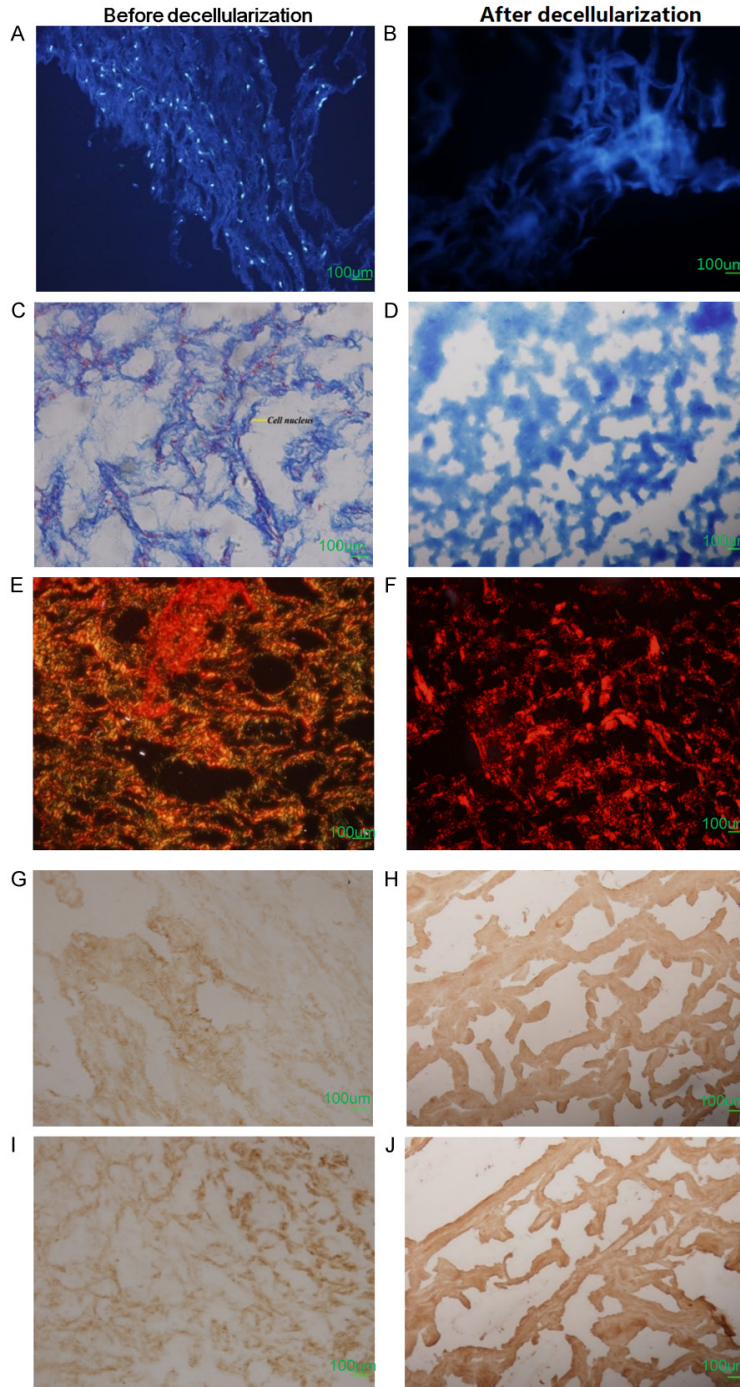


**Figure 3.** The ingredients of WJ-derived ECM before/after decellularization. DAPI fluorescent staining (A, B). Masson stain (C, D). Sirius red stain (E, F). Immunohistochemical stain of type-I collagen (G, H), and type-II collagen (I, J).

stain result showed abundant collagenous fibers (blue) and few elastic fibers (red) in the WJ, and the cell nucleus presented as blue-brown with a short rod-like appearance (**Figure**

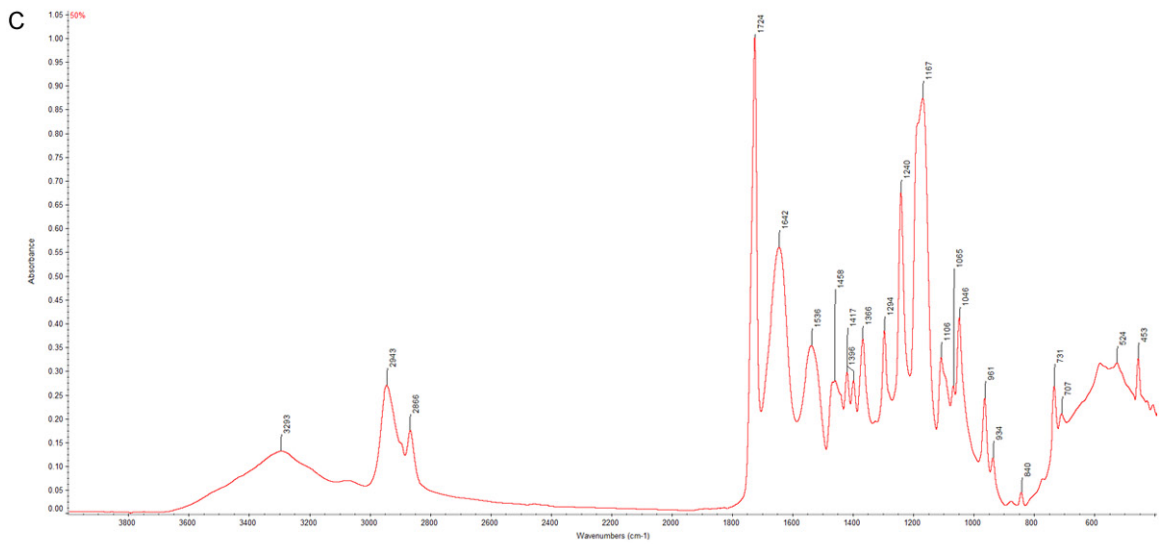
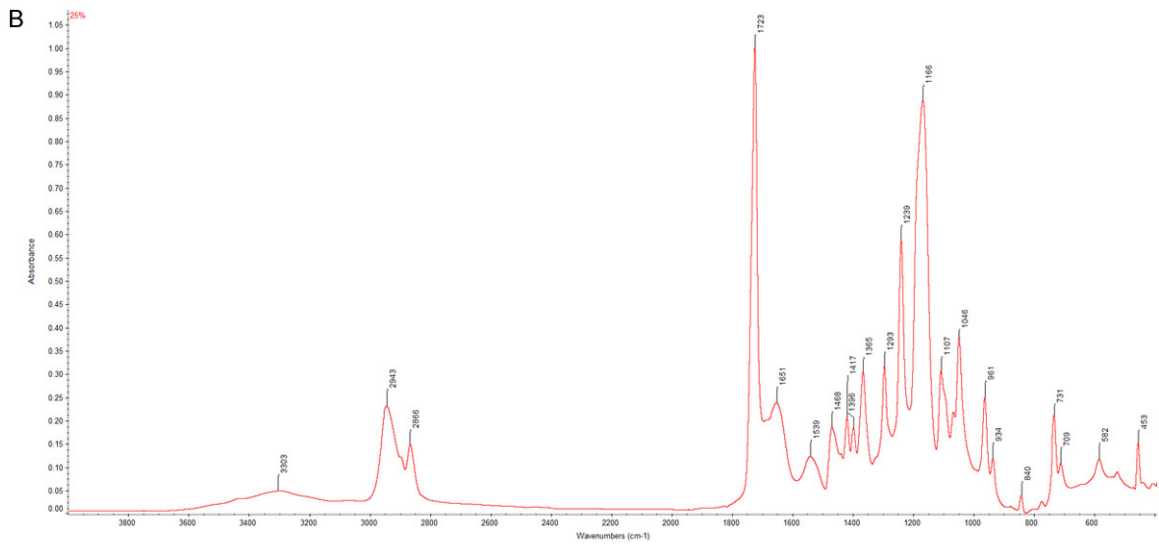
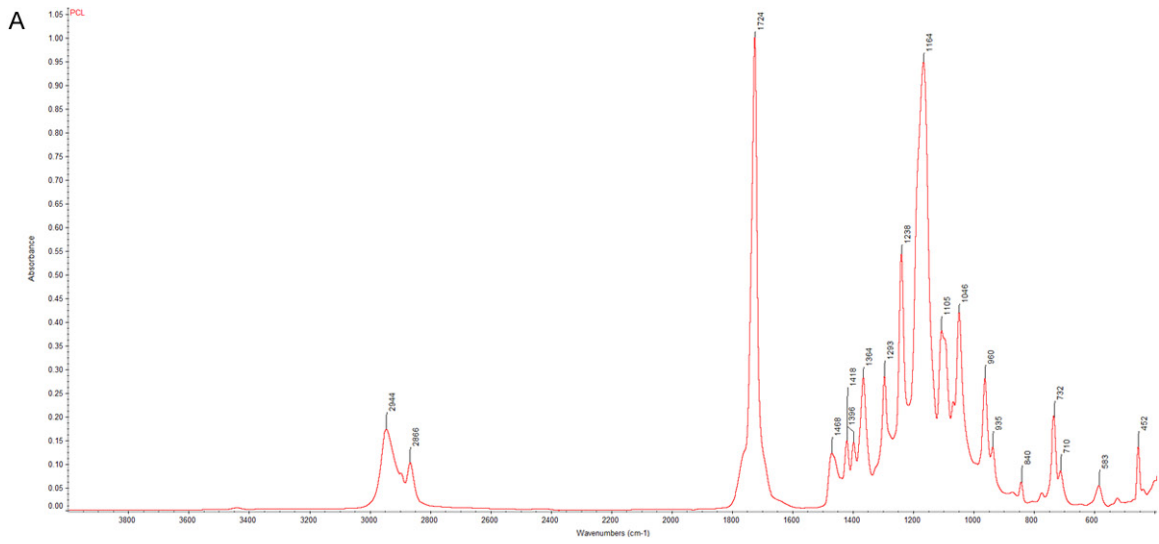
**3C**). The Sirius Red staining results indicated that WJ was full of type I (red and yellow) and type II collagen (colorized), and a small amount of type IV collagen (green) was wrapped with type I collagen (**Figure 3E**). The immunohistochemical staining results also demonstrated that type I and type II collagen existed in the WJ (**Figure 3G, 3I**). After decellularization, the DAPI fluorescent staining result showed WJ-derived ECM without nuclei (**Figure 3B**). The Masson's and Sirius Red stains indicated that the collagen was equally distributed in WJ-derived ECM and that type I collagen was the prime subtype (**Figure 3D and 3F**). The immunohistochemical stain also showed that type I and type II collagen were still present after the decellularization process (**Figure 3H and 3J**).

#### FT-IR results

The FT-IR results showed that PCL ( $\text{CH}_3-(\text{CH}_2)_4-\text{COO}]_n$ ) had two characteristic peaks and many relatively short peaks. In ester bonds,  $\text{C}=\text{O}$  and  $\text{C}-\text{O}-\text{C}$ , respectively, were observed at  $1,723-1,725 \text{ cm}^{-1}$  and  $1,164-1,185 \text{ cm}^{-1}$ ;  $2,943-2,944 \text{ cm}^{-1}$  represented methyl; and  $2,866 \text{ cm}^{-1}$  represented methylene. Other peaks from  $707$  to  $1,468 \text{ cm}^{-1}$  also represented methyl and methylene; however, the vibration modes differed. The two characteristic peak values declined as PCL content decreased and WJ-derived ECM content increased; the other peak values changed little (**Figure 4A**).

Three characteristic peaks belonged to nitrogen-containing compounds in the WJ-derived ECM. Thereinto,  $\text{CO}-\text{N}$  was represented at  $3,291-3,303 \text{ cm}^{-1}$ ,  $\text{N}-\text{H}$  at  $1,530-1,539 \text{ cm}^{-1}$ ,

# Electrospun ECM/PCL band-aid for ATR



## Electrospun ECM/PCL band-aid for ATR

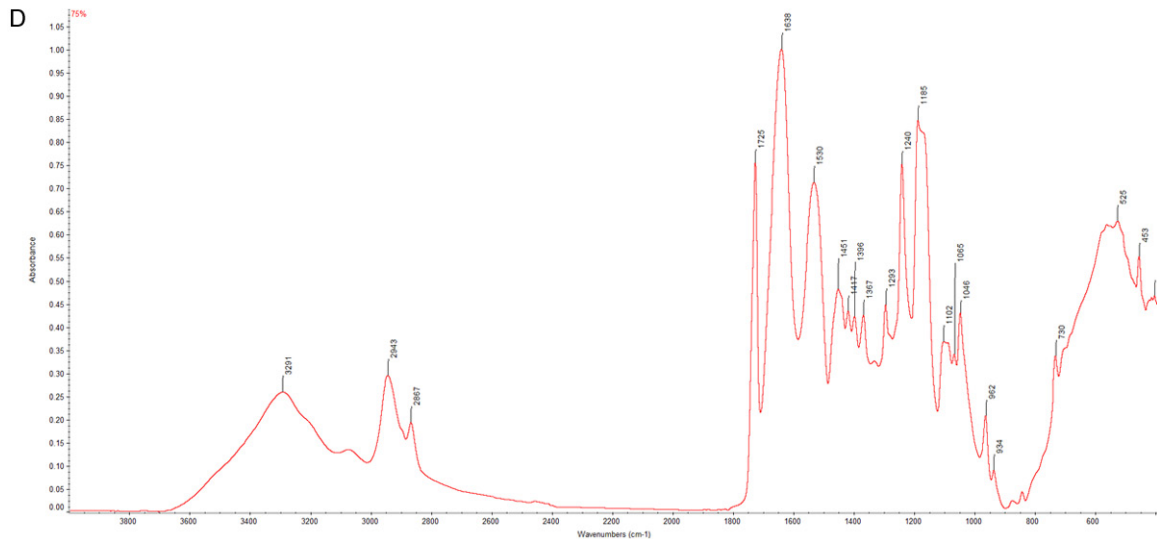


**Figure 4.** The ingredients in electrospun membranes. Dual biomimetic electrospun WJ-derived ECM/PCL sub-micron fibrous band-aid with 0% ECM (A). 25% ECM (B). 50% ECM (C). and 75% ECM (D).

and amido bonds at 1,651-1,638  $\text{cm}^{-1}$ . Furthermore, the three characteristic peaks values indicating the amount of WJ-derived ECM increased (**Figure 4B-D**).

### SEM and WCA result

The fibers were in a parallel arrangement and piled one on top of another in every figure at 6,000  $\times$ . The fibers in pure PCL electrospun membranes were well formed; however, the porosity was inferior (**Figure 5A**). The fibrous arrangement became more disordered as the content of WJ-derived ECM increased, and porosity increased (**Figure 5B-D**).

The WCA value of WJ-derived ECM was less than that of the pure PCL electrospun membrane; the electrospun membrane with 50% WJ-derived ECM and 50% PCL had the best hydrophilicity (**Figure 5A-D**).

The fibrous diameter and WCA values of each group are listed in **Table 1**.

### MTT

The quantities of adhering L929 cells was the electrospun inner layer with 75% ECM > 50% ECM > 25% ECM > 0% ECM > control group on Day 1. Besides, the number of L929 cells on the electrospun inner layers increased, except in the 0% ECM group on Day 4 (**Figure 6**).

### Discussion

In order to solve the complications like re-rupture and adhesion after an ATR, except second operation and rehabilitation therapy [30, 31], many anti-cancer, anti-fibrosis, and anti-infectious drugs, such as chitosan, HA, PLGA and PCL [13, 32-34], have been used to alleviate peritendinous adhesions [17, 35, 36]. In addition, cytokines and stem cells have been used to help improve Achilles tendon healing [15, 37]. However, the dual biomimetic electrospun WJ-derived ECM/PCL sub-micron fibrous band-aid seems to be a progressive solution.

First, WJ-derived ECM has similar ingredients to those in the Achilles tendon. Type I collagen was the basis for the WJ-derived ECM. After the decellularization process, the contents of ingredients decreased, and the proportion of ingredients changed. The microstructure also broke in the WJ-derived ECM. Surprisingly, type I collagen was concentrated and enriched, which was explained by the decellularization process' simulating the Achilles tendon's ECM. FT-IR and SEM demonstrated that the collagen from the WJ-derived ECM was contained in the inner layer of the electrospun band-aid.

Second, the outer layer of the dual biomimetic electrospun WJ-derived ECM/PCL sub-micron fibrous band-aid was compact and parallel,

## Electrospun ECM/PCL band-aid for ATR

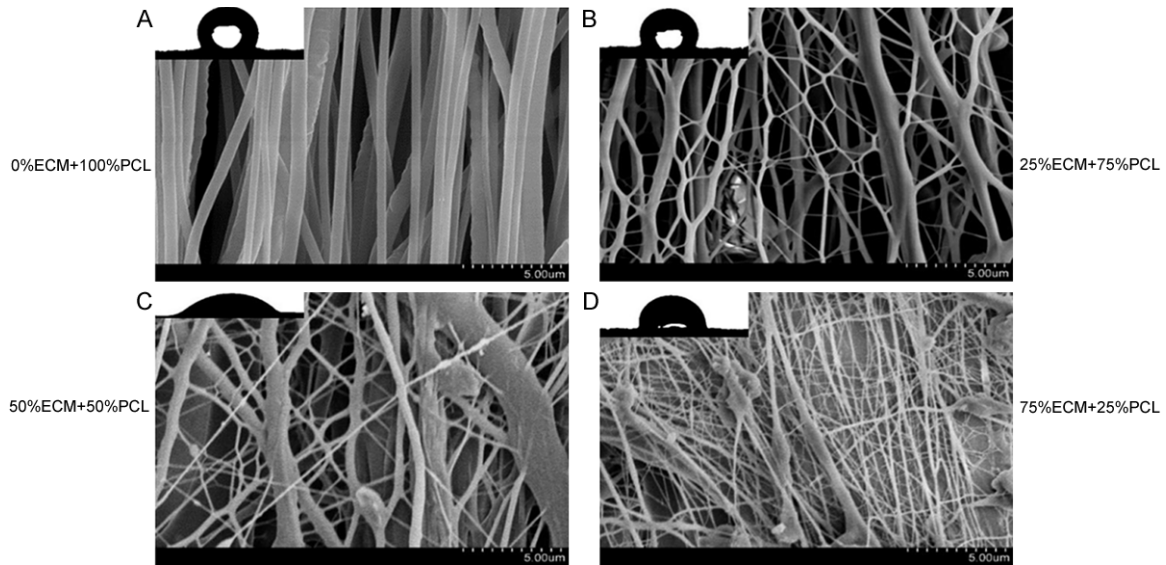


**Figure 5.** The microstructure and water contact angle of electrospun membranes. Dual biomimetic electrospun WJ-derived ECM/PCL sub-micron fibrous band-aid with 0% ECM (A), 25% ECM (B), 50% ECM (C), and 75% ECM (D).

**Table 1.** The fibrous diameters and WCA of dual biomimetic electrospun WJ-derived ECM/PCL sub-micron fibrous band-aids with different ratio of ECM

ECM ratio (g/g)	Fibrous diameter (nm)	Water contact angle (°)
0	478±156	120.38±4.95
25%	348±518 <sup>a</sup>	111.40±3.24
50%	438±166	60.83±2.65 <sup>a</sup>
75%	157±54.3 <sup>a</sup>	89.52±2.51 <sup>a</sup>

<sup>a</sup>P < 0.05 vs. the 0% ECM group.

which was not conducive to cell adhesion or survival, and the inner layer was undulant, poriferous, and similar to the Achilles tendon in fibrous arrangement, which attracts cells to settle and promotes cell proliferation [19].

Third, hydrophilicity, as reflected by WCA, influences cell adhesion. As the WCA decreases, it is easier for cells to adhere to the material [38]. The MTT assay results on the first day showed that the electrospun band-aid with 25% or 50% ECM in the inner layer was better than those without ECM, supporting the viewpoint mentioned above. However, the electrospun band-aid with 75% ECM adhered to fewer cells. The corresponding SEM result showed that the deficiency in PCL led to fibers so slender that the ECM could not be wrapped in PCL fibers. The slender inner layer was unsuitable for adhering

to cells; thus, fewer adhering cells were observed on the electrospun band-aid with 75% ECM than on those with 0% ECM. What's more, the cells quantities on the electrospun membranes were more than control group, which meant the electrospun membranes had better cell adhesive capacity than control group, and the electrospun membranes were without cytotoxicity. On Day 4, the number of L929 cells decreased only on the electrospun band-aid without ECM, whereas the band-aid with 50% ECM had the best cell proliferation, demonstrating that PCL was incompatible with cell proliferation but that the electrospun band-aid with 50% WJ-derived ECM was suitable. Therefore, the dual biomimetic electrospun WJ-derived ECM/PCL sub-micron fibrous band-aid had the ability to prevent peritendinous adhesions through the outer layer and improve regeneration of the Achilles tendon via the inner layer after ATR.

Furthermore, the autologous umbilical cord is not immunologically rejected by the body. Moreover, the decellularization process was performed using a physical method, without enzymes or chemical reagents, and the effect of decellularization was ideal. Therefore, WJ-derived ECM has potential use in the clinic.

In summary, a dual biomimetic electrospun WJ-derived ECM/PCL submicron fibrous band-aid, in which the outer layer contains only PCL

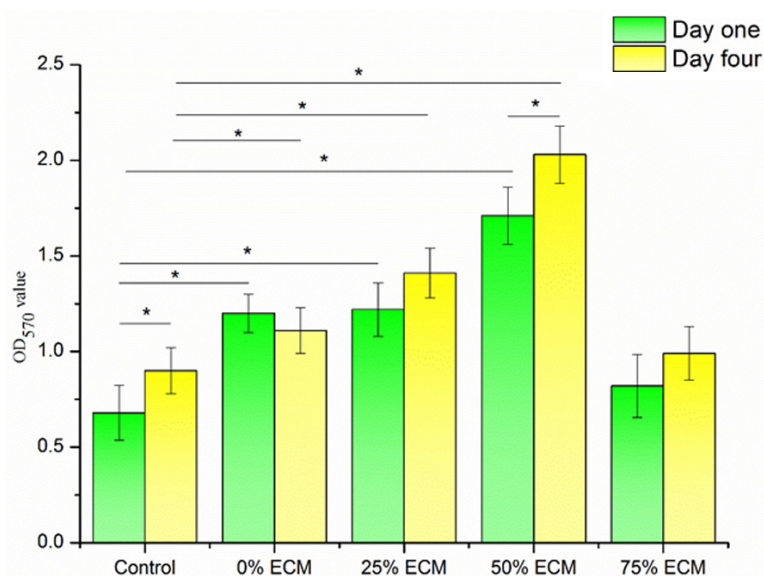


**Figure 6.** The adhesive capacity and viability of L929 fibroblasts on the electrospun membranes.

and the inner layer includes 50% ECM and 50% PCL, was developed. The outer layer inhibited cell survival, and the inner layer promoted cell adherence and proliferation *in vitro*. Hence, this band-aid may have the ability to prevent peritendinous adhesions and re-rupture after ATR.

#### Acknowledgements

This study was funded by the National Natural Science Foundation of China (21134004); High Technology Research and Development Program of China (2012AA020502, 2015AA020303), and Beijing Science and Technology Development (Z161100005016059). The authors are indebted to the pregnant women in the obstetrics department at Chinese PLA General Hospital for kindly providing the umbilical cords.

#### Disclosure of conflict of interest

None.

**Address correspondence to:** Quanyi Guo, Beijing Key Laboratory of Regenerative Medicine in Orthopaedics, Key Laboratory of Musculo-Skeletal Trauma & War Injuries, PLA, Institute of Orthopaedics, Chinese PLA General Hospital, 28 Fuxing Road, Haidian District, Beijing 100853, China. Tel: +86 15810335479; Fax: +861066939205; E-mail: doc-torguo\_301@163.com

#### References

- [1] De la Fuente CI, Lillo RP, Ramirez-Campillo R, Ortega-Auriol P, Delgado M, Alvarez-Ruf J and Carreno G. Medial gastrocnemius myotendinous junction displacement and plantar-flexion strength in patients treated with immediate rehabilitation after Achilles tendon repair. *J Athl Train* 2016; 51: 1013-1021.
- [2] Kearney RS, McGuinness KR, Achten J and Costa ML. A systematic review of early rehabilitation methods following a rupture of the Achilles tendon. *Physiotherapy* 2012; 98: 24-32.
- [3] Groetelaers RP, Janssen L, van der Velden J, Wieland AW, Amendt AG, Geelen PH and Janzing HM. Functional treatment or cast immobilization after minimally invasive repair of an acute Achilles tendon rupture: prospective, randomized trial. *Foot Ankle Int* 2014; 35: 771-778.
- [4] Jielile J, Badalihan A, Qianman B, Satewalede T, Wuerliebieke J, Kelamu M and Jialihasi A. Clinical outcome of exercise therapy and early post-operative rehabilitation for treatment of neglected Achilles tendon rupture: a randomized study. *Knee Surg Sports Traumatol Arthrosc* 2016; 24: 2148-2155.
- [5] Metz R, Kerkhoffs GM, Verleisdonk EJ and van der Heijden GJ. Acute Achilles tendon rupture: minimally invasive surgery versus non operative treatment, with immediate full weight bearing. Design of a randomized controlled trial. *BMC Musculoskelet Disord* 2007; 8: 108.
- [6] MacMahon A, Deland JT, Do H, Soukup DS, Sofka CM, Demetracopolous CA and DeBlis R. MRI evaluation of Achilles tendon rotation and sural nerve anatomy: implications for percutaneous and limited-open Achilles tendon repair. *Foot Ankle Int* 2016; 37: 636-643.
- [7] Makulavicius A, Martin Oliva X, Mazarevicius G, Klinga M, Uvarovas V, Porvaneckas N, Monzo Planella M and Mazurek T. Comparative anatomical study of standard percutaneous and modified medialised percutaneous Bunnell type repair for artificial Achilles tendon rupture: positive effect of medialisation of the stitches with lower risk of sural nerve injury. *Folia Morphol (Warsz)* 2016; 75: 53-59.
- [8] Keyhani S, Mardani-Kivi M, Abbasian M, Emami-Moghaddam Tehrani M and Lahiji FA. Achil-

- les tendon repair, a modified technique. *Arch Bone Jt Surg* 2013; 1: 86-89.
- [9] Miyamoto W, Imade S, Innami K, Kawano H and Takao M. Acute Achilles tendon rupture treated by double side-locking loop suture technique with early rehabilitation. *Foot Ankle Int* 2017; 38: 167-173.
- [10] Badalihan A, Aihemaiti A, Shawutali N, Jielile J, Jialihasi A, Tangkejie W, Nuerdoula Y, Satewalede T, Hunapiya B, Niyazebieke H, Hezibieke H, Zhao Q, Bahetijiang A, Kelamu M and Qianman B. Outcome of a one-stage tensile stress surgical technique and early postoperative rehabilitation in the treatment of neglected Achilles tendon rupture. *J Foot Ankle Surg* 2015; 54: 153-159.
- [11] Ishiyama N, Moro T, Ishihara K, Ohe T, Miura T, Konno T, Ohyama T, Kimura M, Kyomoto M, Nakamura K and Kawaguchi H. The prevention of peritendinous adhesions by a phospholipid polymer hydrogel formed in situ by spontaneous intermolecular interactions. *Biomaterials* 2010; 31: 4009-4016.
- [12] Chen Q, Lu H and Yang H. Chitosan inhibits fibroblasts growth in Achilles tendon via TGF-beta1/Smad3 pathway by miR-29b. *Int J Clin Exp Pathol* 2014; 7: 8462-8470.
- [13] Yuan F, Lin LX, Zhang HH, Huang D and Sun YL. Effect of carbodiimide-derivatized hyaluronic acid gelatin on preventing postsurgical intra-abdominal adhesion formation and promoting healing in a rat model. *J Biomed Mater Res A* 2016; 104: 1175-1181.
- [14] Tosun HB, Gumustas SA, Kom M, Uludag A, Serbest S and Eroksuz Y. The effect of sodium hyaluronate plus sodium chondroitin sulfate solution on peritendinous adhesion and tendon healing: an experimental study. *Balkan Med J* 2016; 33: 258-266.
- [15] Guerquin MJ, Charvet B, Nourissat G, Havis E, Ronsin O, Bonnin MA, Ruggiu M, Olivera-Martinez I, Robert N, Lu Y, Kadler KE, Baumberger T, Doursounian L, Berenbaum F and Duprez D. Transcription factor EGR1 directs tendon differentiation and promotes tendon repair. *J Clin Invest* 2013; 123: 3564-3576.
- [16] Zhao X, Jiang S, Liu S, Chen S, Lin ZY, Pan G, He F, Li F, Fan C and Cui W. Optimization of intrinsic and extrinsic tendon healing through controllable water-soluble mitomycin-C release from electrospun fibers by mediating adhesion-related gene expression. *Biomaterials* 2015; 61: 61-74.
- [17] Liu S, Zhao J, Ruan H, Wang W, Wu T, Cui W and Fan C. Antibacterial and anti-adhesion effects of the silver nanoparticles-loaded poly (L-lactide) fibrous membrane. *Mater Sci Eng C Mater Biol Appl* 2013; 33: 1176-1182.
- [18] Chen S, Wang G, Wu T, Zhao X, Liu S, Li G, Cui W and Fan C. Silver nanoparticles/ibuprofen-loaded poly (L-lactide) fibrous membrane: anti-infection and anti-adhesion effects. *Int J Mol Sci* 2014; 15: 14014-14025.
- [19] Zhang W, Zhu Y, Li J, Guo Q, Peng J, Liu S, Yang J and Wang Y. Cell-derived extracellular matrix: basic characteristics and current applications in orthopedic tissue engineering. *Tissue Eng Part B Rev* 2016; 22: 193-207.
- [20] Yin H, Wang Y, Sun Z, Sun X, Xu Y, Li P, Meng H, Yu X, Xiao B, Fan T, Wang Y, Xu W, Wang A, Guo Q, Peng J and Lu S. Induction of mesenchymal stem cell chondrogenic differentiation and functional cartilage microtissue formation for in vivo cartilage regeneration by cartilage extracellular matrix-derived particles. *Acta Biomater* 2016; 33: 96-109.
- [21] Yuan Z, Liu S, Hao C, Guo W, Gao S, Wang M, Chen M, Sun Z, Xu Y, Wang Y, Peng J, Yuan M and Guo QY. AMECM/DCB scaffold prompts successful total meniscus reconstruction in a rabbit total meniscectomy model. *Biomaterials* 2016; 111: 13-26.
- [22] Franc S, Rousseau JC, Garrone R, van der Rest M and Moradi-Ameli M. Microfibrillar composition of umbilical cord matrix: characterization of fibrillin, collagen VI and intact collagen V. *Placenta* 1998; 19: 95-104.
- [23] Jadalannagari S, Converse G, McFall C, Buse E, Filla M, Villar MT, Artigues A, Mellot AJ, Wang J, Detamore MS, Hopkins RA and Aljitiw OS. Decellularized Wharton's Jelly from human umbilical cord as a novel 3D scaffolding material for tissue engineering applications. *PLoS One* 2017; 12: e0172098.
- [24] Chen SH, Chen CH, Shalumon KT and Chen JP. Preparation and characterization of antiadhesion barrier film from hyaluronic acid-grafted electrospun poly (caprolactone) nanofibrous membranes for prevention of flexor tendon postoperative peritendinous adhesion. *Int J Nanomedicine* 2014; 9: 4079-4092.
- [25] Dankers PY, Boomker JM, Huizinga-van der Vlag A, Wisse E, Appel WP, Smedts FM, Harmen MC, Bosman AW, Meijer W and van Luyn MJ. Bioengineering of living renal membranes consisting of hierarchical, bioactive supramolecular meshes and human tubular cells. *Biomaterials* 2011; 32: 723-733.
- [26] Martinez C, Fernandez C, Prado M, Ozols A and Olmedo DG. Synthesis and characterization of a novel scaffold for bone tissue engineering based on Wharton's jelly. *J Biomed Mater Res A* 2017; 105: 1034-1045.
- [27] Liu S, Zhao J, Ruan H, Tang T, Liu G, Yu D, Cui W and Fan C. Biomimetic sheath membrane via electrospinning for antiadhesion of re-

## Electrospun ECM/PCL band-aid for ATR

- paired tendon. *Biomacromolecules* 2012; 13: 3611-3619.
- [28] Chen CH, Chen SH, Shalumon KT and Chen JP. Dual functional core-sheath electrospun hyaluronic acid/polycaprolactone nanofibrous membranes embedded with silver nanoparticles for prevention of peritendinous adhesion. *Acta Biomater* 2015; 26: 225-235.
- [29] Chen CH, Chen SH, Shalumon KT and Chen JP. Prevention of peritendinous adhesions with electrospun polyethylene glycol/polycaprolactone nanofibrous membranes. *Colloids Surf B Biointerfaces* 2015; 133: 221-230.
- [30] Kauwe M. Acute Achilles tendon rupture: clinical evaluation, conservative management, and early active rehabilitation. *Clin Podiatr Med Surg* 2017; 34: 229-243.
- [31] Maffulli N, Oliva F, Del Buono A, Florio A and Maffulli G. Surgical management of Achilles tendon re-ruptures: a prospective cohort study. *Int Orthop* 2015; 39: 707-714.
- [32] Deepthi S, Nivedhitha Sundaram M, Deepti Kadavan J and Jayakumar R. Layered chitosan-collagen hydrogel/aligned PLLA nanofiber construct for flexor tendon regeneration. *Carbohydr Polym* 2016; 153: 492-500.
- [33] Inui A, Kokubu T, Makino T, Nagura I, Toyokawa N, Sakata R, Kotera M, Nishino T, Fujioka H and Kurosaka M. Potency of double-layered poly L-lactic acid scaffold in tissue engineering of tendon tissue. *Int Orthop* 2010; 34: 1327-1332.
- [34] Jiang S, Yan H, Fan D, Song J and Fan C. Multi-layer electrospun membrane mimicking tendon sheath for prevention of tendon adhesions. *Int J Mol Sci* 2015; 16: 6932-6944.
- [35] Jiang S, Zhao X, Chen S, Pan G, Song J, He N, Li F, Cui W and Fan C. Down-regulating ERK1/2 and SMAD2/3 phosphorylation by physical barrier of celecoxib-loaded electrospun fibrous membranes prevents tendon adhesions. *Biomaterials* 2014; 35: 9920-9929.
- [36] Xia C, Zuo J, Wang C and Wang Y. Tendon healing in vivo: effect of mannose-6-phosphate on flexor tendon adhesion formation. *Orthopedics* 2012; 35: e1056-1060.
- [37] Uysal CA, Tobita M, Hyakusoku H and Mizuno H. Adipose-derived stem cells enhance primary tendon repair: biomechanical and immunohistochemical evaluation. *J Plast Reconstr Aesthet Surg* 2012; 65: 1712-1719.
- [38] Qian Y, Chen H, Xu Y, Yang J, Zhou X, Zhang F and Gu N. The preosteoblast response of electrospinning PLGA/PCL nanofibers: effects of biomimetic architecture and collagen I. *Int J Nanomedicine* 2016; 11: 4157-4171.